

## Retraction

# Retracted: Ultrasound Image-Guided Pudendal Nerve Block on Analgesic Effect of Perineotomy under Optimized Fast Super Resolution Reconstructed Convolutional Neural Network Algorithm

### Scientific Programming

Received 17 October 2023; Accepted 17 October 2023; Published 18 October 2023

Copyright © 2023 Scientific Programming. This is an open access article distributed under the Creative Commons Attribution License, which permits unrestricted use, distribution, and reproduction in any medium, provided the original work is properly cited.

This article has been retracted by Hindawi following an investigation undertaken by the publisher [1]. This investigation has uncovered evidence of one or more of the following indicators of systematic manipulation of the publication process:

- (1) Discrepancies in scope
- (2) Discrepancies in the description of the research reported
- (3) Discrepancies between the availability of data and the research described
- (4) Inappropriate citations
- (5) Incoherent, meaningless and/or irrelevant content included in the article
- (6) Peer-review manipulation

The presence of these indicators undermines our confidence in the integrity of the article's content and we cannot, therefore, vouch for its reliability. Please note that this notice is intended solely to alert readers that the content of this article is unreliable. We have not investigated whether authors were aware of or involved in the systematic manipulation of the publication process.

Wiley and Hindawi regrets that the usual quality checks did not identify these issues before publication and have since put additional measures in place to safeguard research integrity.

We wish to credit our own Research Integrity and Research Publishing teams and anonymous and named external researchers and research integrity experts for contributing to this investigation.

The corresponding author, as the representative of all authors, has been given the opportunity to register their

agreement or disagreement to this retraction. We have kept a record of any response received.

### References

- [1] S. Zhang, X. Zhao, G. Zhao, L. Zhang, and Y. Xiu, "Ultrasound Image-Guided Pudendal Nerve Block on Analgesic Effect of Perineotomy under Optimized Fast Super Resolution Reconstructed Convolutional Neural Network Algorithm," *Scientific Programming*, vol. 2021, Article ID 4768673, 8 pages, 2021.

## Research Article

# Ultrasound Image-Guided Pudendal Nerve Block on Analgesic Effect of Perineotomy under Optimized Fast Super Resolution Reconstructed Convolutional Neural Network Algorithm

Shanni Zhang <sup>1</sup>, Xiaoying Zhao <sup>1</sup>, Guixu Zhao <sup>2</sup>, Linyi Zhang <sup>1</sup>, and Yufang Xiu <sup>1</sup>

<sup>1</sup>Department of Anesthesia, Dalian Maternal and Child Health Care Center, Dalian 116021, China

<sup>2</sup>Department of Gynaecology and Obstetrics, Dalian Maternal and Child Health Care Center, Dalian 116021, China

Correspondence should be addressed to Yufang Xiu; 2020160649@stu.cpu.edu.cn

Received 28 August 2021; Revised 29 September 2021; Accepted 4 October 2021; Published 12 November 2021

Academic Editor: Gustavo Ramirez

Copyright © 2021 Shanni Zhang et al. This is an open access article distributed under the Creative Commons Attribution License, which permits unrestricted use, distribution, and reproduction in any medium, provided the original work is properly cited.

This work was aimed to study the analgesic effect of pudendal nerve block on obstetrics and gynecology under the guidance of ultrasound image based on optimized fast super resolution reconstructed convolutional neural network (FSRCNN) algorithm. A total of 110 primiparas from hospital who gave birth through vagina were randomly rolled into experimental group (55 cases) and control group (55 cases). The optimized FSRCNN algorithm was constructed, compared with the FSRCNN algorithm and the Bicubic algorithm and applied to 110 cases of maternal patients undergoing perineotomy under ultrasound image-guided pudendal nerve block. Visual analogue scoring (VAS), incision suture pain VAS score, occurrence of complications, puerpera labor time, and newborn weight were recorded and compared, so did Apgar score of newborns, numbness of maternal thigh, recovery of puncture site, and satisfaction of maternal analgesia. The results showed that the peak signal-to-noise ratio (PSNR) of the high-resolution image reconstructed by the FSRCNN algorithm was 32.68 dB and that reconstructed by the optimized FSRCNN algorithm was 32.19 dB. The PSNR of the Bicubic algorithm processed image was 28.51 dB. In the lateral resection of episiotomy in the second stage of labor, the visual analog score ( $2.3 \pm 1.5$  points) of the experimental group was inferior to that of the control group ( $7.1 \pm 2.6$  points) ( $P < 0.05$ ). The visual analogue score of stitch pain ( $1.3 \pm 0.8$  points) was also inferior to that of the control group ( $5.2 \pm 1.9$  points) ( $P < 0.05$ ). Moreover, the satisfaction of the parturients in the experimental group ( $9.86 \pm 0.41$  points) was considerably superior to that of the control group ( $7.36 \pm 1.25$  points) ( $P < 0.05$ ). In short, the optimized FSRCNN algorithm had a short training time and good reconstruction effect. Ultrasound-guided pudendal nerve block had a substantial analgesic effect on the second stage of labor and improved parturients' satisfaction.

## 1. Introduction

Perineotomy is a surgical incision in the perineum and the posterior wall of the vagina, usually performed by a midwife or obstetrician [1]. Perineotomy is usually performed in the second stage of labor to rapidly widen the opening through which the baby passes. Perineotomy has been accepted as medical practice in various countries for many years, and it has been rapidly gaining popularity among obstetricians and midwives since the 1960s in almost all countries in Europe, Australia, Canada, and the United States [2]. According to the investigation and research, there are obvious differences between Chinese women and European and American

women in the pelvis. The proportion of Chinese women who underwent lateral resection during the first delivery is 96%, whereas that in European and American countries is only 52% [3].

During the first and second stages of labor, the fetus's descent in the birth canal will cause compression on the vagina and perineum, and the expansion of the birth canal will lead to strong stretching and tearing of fascia and subcutaneous tissues [4]. The pudendal nerve, originating from S2, S3, and S4, spans the highest point of the sciatic spine, crosses between the sacrospinous ligament and the spinous tuberos ligament, and gives off three branches of the inferior rectum nerve, the perineal nerve, and the dorsal

penis/clitoral nerve, which are mainly responsible for supplying the perineum [5]. Vaginal nerve block must be perfected if physical pain due to stretching of the vaginal and perineal structures is to be prevented. Vaginal nerve blocks block the transmission of perineal pain, allowing pelvic floor muscle tissue to relax completely. It can not only relieve labor pain but also reduce the resistance of fetal delivery, shorten the time of the second stage of labor, and have no effect on uterine autonomic nerve and uterine contractions [6].

Traditional pudendal nerve block uses blind detection, which can easily damage women's pudendal arteries and veins, causing hematoma or local anesthetic poisoning [7]. With the continuous development of imaging technology, perineotomy under the guidance of ultrasound images can not only show the layers of the tissues but also reduce the risk of pudendal nerve block [8]. Yao et al. [9] reported that the use of an ultrasound probe to move along the pudendal nerve in the human body for translation can clearly show the pudendal nerve at all levels. Liu et al. [10] proposed the fast super resolution reconstructed convolutional neural network (FSRCNN) algorithm in 2018. The network structure is improved. By inputting low-resolution images and using deconvolution layer to realize upsampling, better super-resolution quality can be obtained than existing methods, and the speed is dozens of times faster, which can improve the reconstruction effect of ultrasonic images.

In this study, the optimized FSRCNN algorithm was constructed, compared with the FSRCNN algorithm and the Bicubic algorithm, and applied to 110 cases of female delivery patients undergoing perineotomy under ultrasound image-guided pudendal nerve block. By comparing the analgesic effects of pudendal nerve block patients in the experimental group and epidural analgesia patients in the control group, the superiority of ultrasound image-guided pudendal nerve block was explored, hoping to provide reliable evidence for obstetrics and gynecology delivery treatment.

## 2. Materials and Methods

**2.1. Research Object.** In this study, 110 primiparas who delivered naturally through vagina in hospital from October 2018 to November 2020 were recruited. They were randomly divided into experimental group (55 cases) and control group (55 cases), with an average age of  $25.69 \pm 5.47$  years. This study had been approved by the Ethics Committee of hospital, and the included subjects or their family members had signed the informed consent.

Inclusion criteria are as follows: (i) patients aged between 22 and 35 years old; (ii) single fetus, first delivery, and first exposure; (iii) body mass index (BMI) of  $20\text{--}32\text{ kg/m}^2$ ; (iv) the gestational age was between 37 and 42 weeks.

Exclusion criteria were (i) patients with complicated mental illness; (ii) patients combined with scoliosis; (iii) patients with abnormal coagulation function; (iv) patients complicated with hypertension, hyperglycemia, or diabetes; (v) patients with smoking, drinking, and other bad behaviors.

**2.2. Analgesic Methods.** The epidural analgesia method in the control group was as follows. The side decubitus position was taken for the puerpera, and epidural puncture site was usually selected for lumbar 2–3 space or lumbar 3–4 space. The experimental dose was 3 mL 15% lidocaine containing 1:200,000 epinephrine. The catheter was inserted into the epidural space through the puncture needle. When the catheter passed 3–5 cm through the tip, one hand was placed against the catheter and the other hand was pulled out of the epidural needle. The appropriate indwelling length of the catheter in the epidural space was 3–4 cm. If the resistance of the catheter passing through the tip was large during catheterization, the puncture needle was rotated or try to insert the catheter after a little insertion. To reduce the risk of catheter placement into blood vessels, 5–75 mL of normal saline was injected before catheterization, and catheterization was conducted during the intermission period of contractions. The setting mode of analgesia pump was epidural intermittent pulse infusion.

In the experimental group, the pudendal nerve block under the guidance of ultrasound was as follows. The puerpera took the prone position. Clover 60 T portable color ultrasound diagnostic instrument (Guangdong Goworld Co., Ltd., China) was used for examination. The low-frequency convex array C5-1 ultrasonic probe (Guangdong Goworld Co., Ltd., China) was used for cross-sectional scanning, forming ischium notch. The probe was moved from head to tail, and the ischium appeared as a gradually lengthened hyperechoic linear shadow, which was the widest at the level of the ischium spine. The sacrospinous ligament and ischium spine presented continuous hyperechoic linear shadow, and the echo was slightly inferior to that of bone. The sacrotuberous ligament, as a slight hyperechoic linear shadow deep in the gluteus maximus, was parallel to the sacrospinous ligament. Doppler imaging showed the internal pudendal artery near the ischium spine. A 22 G lumbar anesthesia needle or nerve stimulation needle was selected from the inside of the ultrasound probe, and the needle was pierced to the inside of the internal pudendal artery. Inserting the needle from the medial to the lateral side can avoid direct contact with the ischium tubercle and avoid rectal perforation. When the short needle passed through the sacrotuberous ligament, there was a substantial sense of rubber resistance. If there was no blood, 15 mL 0.375% ropivacaine (Chengdu Jiaye Biotechnology Co., Ltd., China) was slowly injected, and the pudendal nerve floated in the liquid.

**2.3. Observation Indexes and Analgesic Effect.** Prior to delivery, the maternal age, gestational age, weight, height, BMI, and other basic information were recorded. The analgesic effect was assessed on a visual analogue scale (VAS) ranging from 0 to 10, with 0 being painless, 1 to 3 being mild, 4 to 6 being moderate, 7 to 9 being severe, and 10 being intolerable. Visual analogue scoring incision suture pain VAS score, and complication incidence were recorded during delivery. The duration of labor, neonatal weight, and neonatal Apgar score were recorded after delivery. After returning to the common

room, the numbness of the maternal thighs, the recovery of the puncture site, and the satisfaction of the maternal analgesic effect were recorded.

#### 2.4. The Construction of the Optimized FSRCNN Algorithm.

The FSRCNN algorithm is a single image superresolution reconstruction algorithm based on convolutional neural network, which is the optimization of the SRCNN algorithm. Figure 1 is a comparison diagram of the FSRCNN algorithm and the SRCNN algorithm. The FSRCNN algorithm mainly includes a three-layer neural network. The first layer performs feature extraction and feature representation corresponding to convolution, the second layer performs nonlinear mapping corresponding to convolution, and the third layer performs convolution corresponding to the final reconstruction.  $X$  is set as the original image, the interpolated image  $Y$  is taken as input, and output is  $G1$ .

$$G1Y = \max(0, A1 \times Y + B1). \quad (1)$$

In formula (1),  $A1$  represents the convolution kernel,  $B1$  represents the weight bias, and  $G1(Y)$  represents the output image.  $A1$  is composed of  $m \times c1 \times h1 \times h1$  convolution kernels, where  $c1$  represents the number of channels, and  $B1$  is  $m1$  offsets. The last adjusted parameters are  $h1 = 10$  and  $h1 = 65$ . The second layer of convolutional neural network is based on the  $m1$  feature maps generated by the first layer and is mapped into  $m2$  feature maps. The calculation formula is as follows.

$$G2Y = \max(0, A2 \times G2(Y) + B2). \quad (2)$$

In formula (2),  $A2$  represents the convolution kernel,  $B2$  represents the weight bias, and  $G2(Y)$  represents the output image.  $A2$  is composed of  $m2 \times n1 \times h2 \times h2$  convolution kernels,  $B2$  is  $m2$  offsets, and the values are  $h2 = 1$  and  $n2 = 32$ . The third layer is the reconstruction layer, and the formula for establishing the reconstruction layer is as follows.

$$G(Y) = A3 \times G2(Y) + B3. \quad (3)$$

In formula (3),  $A3$  is composed of  $c \times m2 \times h3 \times h3$  convolution kernels, and  $B3$  is  $c$  offsets, where the value  $c = 3$ ,  $h3 = 5$ .

To improve the image superresolution, FSRCNN algorithm was optimized based on the reduced reconstruction speed, and a dual optimization of reconstruction speed and reconstruction quality was explored. First, the feature extraction layer of the FSRCNN algorithm has only one layer. The optimization is carried out for the defect of inaccurate features of the single convolutional layer adopted by the FSRCNN algorithm. A convolution layer of feature extraction is added. The two-layer feature extraction is adopted, and the parameters of the network are optimized, increasing the depth of the network layer and modifying the size of the convolution kernel, which can considerably improve the accuracy of image feature extraction. To reduce the randomness of FSRCNN algorithm in the process of image reconstruction, the deconvolution layer is placed in front of feature extraction by changing the network

structure. After the image is enlarged, the feature extraction in the training process is carried out to further improve the accuracy of image feature extraction. Figure 2 is the schematic diagram of the optimized FSRCNN algorithm.

2.5. *Optimized Fast Superresolution Ultrasound Image Reconstruction Experiment.* In this experiment, the bicubic interpolation experiment of the test set was used as the experimental comparison index, and the FSRCNN algorithm before optimization and the optimized FSRCNN algorithm were trained with different times of iteration. The peak signal-to-noise ratio (PSNR) of different iteration times was calculated and compared with the image reconstructed by Bicubic algorithm. Ultrasound-guided images of pudendal nerve block were used for each iteration.

2.6. *Statistical Methods.* SPSS 22.0 was employed for data statistics and analysis. Mean  $\pm$  standard deviation ( $\bar{x} \pm s$ ) was how measurement data were expressed, and the  $t$ -test was used to compare the mean values between the groups. Percentage (%) was how count data were expressed. The difference was statistically considerable with  $P < 0.05$ .

## 3. Results

3.1. *Experimental Results of the Optimized FSRCNN Algorithm.* Figure 3 shows the comparison of reconstruction effects of different algorithms. In this experiment, PSNR was selected as a quantitative index of image reconstruction effect. The PSNR of the high-resolution image reconstructed by the FSRCNN algorithm was 32.68 dB, the PSNR of the high-resolution image reconstructed by the optimized FSRCNN algorithm was 32.19 dB, and the PSNR of the Bicubic algorithm processed image was 28.51 dB. It showed that increasing the number of convolutional layers can make the neural network become deeper, improve the performance of the model, and make the reconstruction results accurate. The FSRCNN algorithm got  $5 \times 10^6$  iterations after training for about 200h. The optimized FSRCNN algorithm reached  $5 \times 10^6$  iterations after training for about 650h. The above data showed that the optimized FSRCNN algorithm was superior to the FSRCNN algorithm and the Bicubic algorithm in terms of training time and reconstruction effect.

3.2. *General Information of Parturient.* Figure 4 shows the comparison of general information of the parturient. The average age of parturient in the experimental group was  $25.4 \pm 4.1$  years, and the average height was  $157.3 \pm 4.5$  cm. The average age of parturient in the control group was  $26.3 \pm 3.8$  years, and the average height was  $162.4 \pm 3.4$  cm. There was no substantial difference between the two groups ( $P > 0.05$ ). In addition, the average gestational week of the parturient in experimental group was  $37.2 \pm 0.75$  weeks, and the BMI was  $25.8 \pm 3.1 \text{ kg/m}^2$ . The average gestational week of the parturient in control group was  $37.4 \pm 0.81$  weeks, and the BMI was  $26.4 \pm 3.4 \text{ kg/m}^2$ . There was no substantial

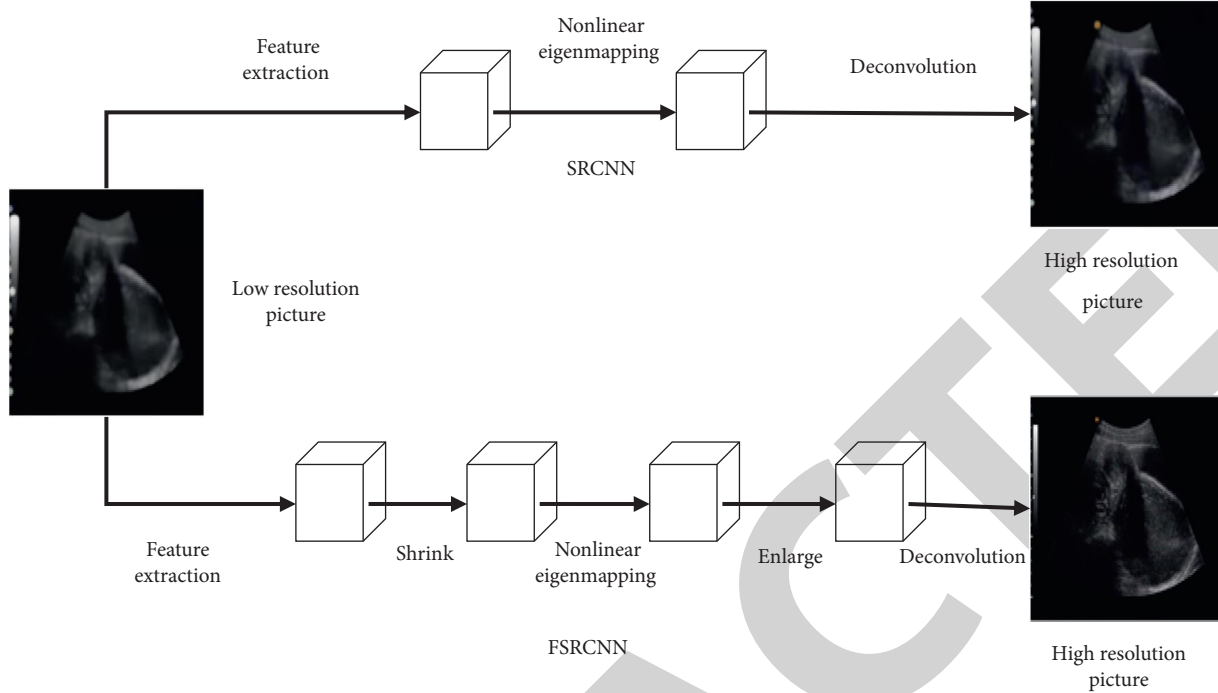


FIGURE 1: Comparison of FSRCNN algorithm and SRCNN algorithm.

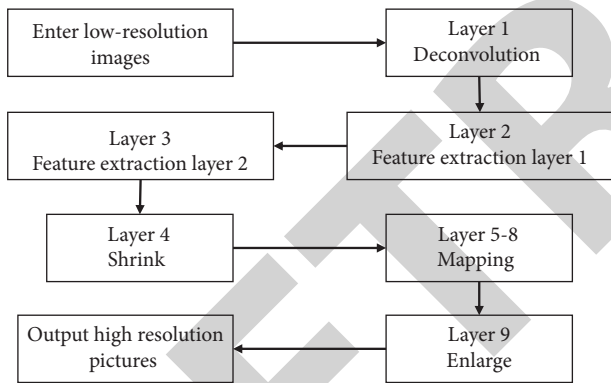


FIGURE 2: Schematic diagram of the optimized FSRCNN algorithm.

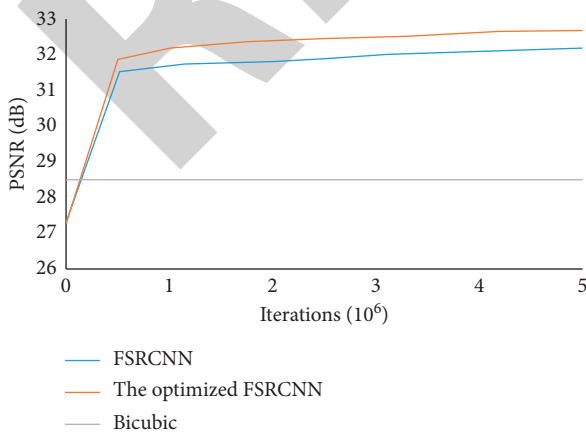


FIGURE 3: Comparison of reconstruction effects of different algorithms.

difference between the two groups ( $P > 0.05$ ). The above data showed that the two groups of parturient were comparable.

3.3. *Ultrasound Images.* Doppler ultrasound image in Figure 5 shows the right pudendal artery and pudendal nerve. Doppler ultrasound was used to locate the sacrotuberous ligament, the sacrospinous ligament, and the sciatic tubercle. The brown muscle covering the surface of the sciatic tubercle was the obturator internus muscle. The location of the pudendal nerve block at the level of the sciatic was high, which was close to the sciatic nerve. The pudendal nerve was located in the triangular region surrounded by the sacrotuberous ligament, the sacrospinous ligament, and the obturator internus muscle. Doppler ultrasound can reveal the internal pudendal artery and indicate the location of the pudendal nerve.

3.4. *Comparison of Analgesic Effects.* Figure 6 shows the comparison of the analgesic effects of the parturients during the various stages of labor. There was no substantial difference in the VAS scores of the two groups of parturients before and after epidural anesthesia in the first stage of labor ( $P > 0.05$ ). In the lateral resection of episiotomy in the second stage of labor, the VAS score of the parturients in experimental group ( $2.3 \pm 1.5$  points) was inferior to that of the control group ( $7.1 \pm 2.6$  points), with substantial difference ( $P < 0.05$ ). The VAS score ( $1.3 \pm 0.8$  points) of stitch pain was inferior to that of the control group ( $5.2 \pm 1.9$  points), with substantial difference ( $P < 0.05$ ). The proportion of parturients who received additional local anesthesia infiltration in the experimental group (10.91%) was considerably inferior to that of the control group (16.36%), with

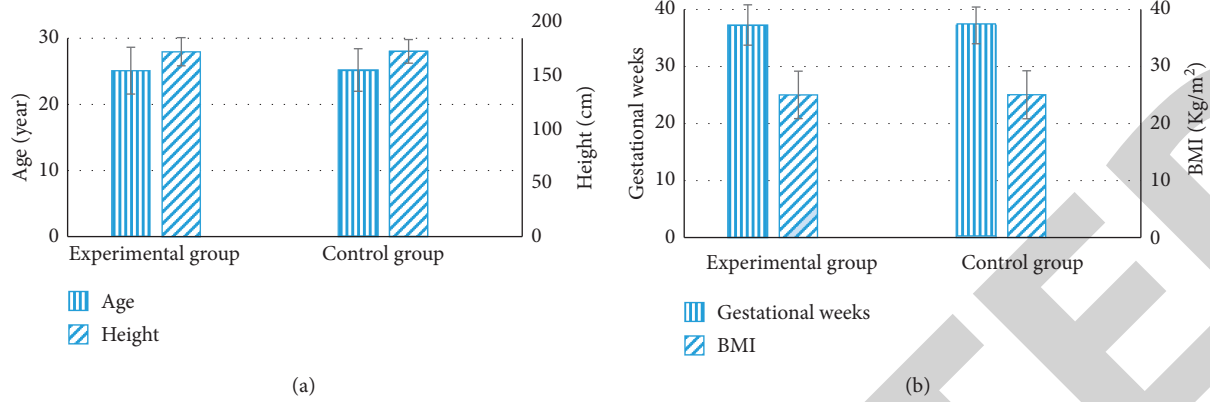


FIGURE 4: Comparison of general information of parturients. (a) Comparison of age and height between the experimental group and the control group; (b) comparison of gestational age and BMI between the experimental group and the control group.

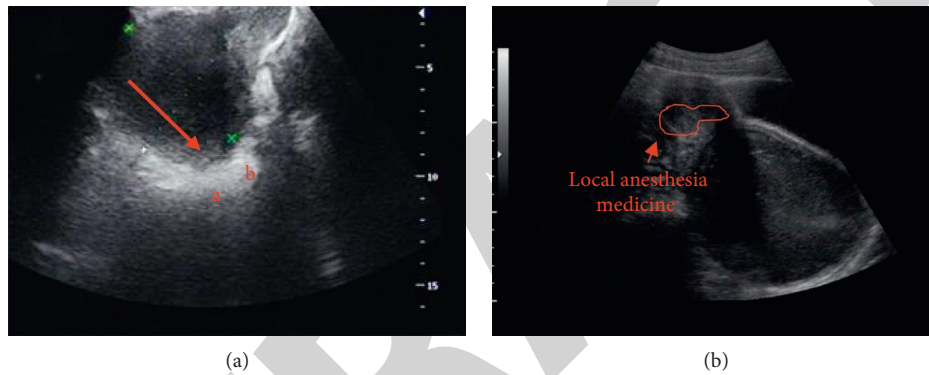


FIGURE 5: Ultrasound images of pudendal nerve block. (a) The pudendal artery and pudendal nerve on the right. Ischial spine level, no anesthetic injection, a indicates the right pudendal nerve, b indicates the pudendal artery, and the arrow indicated the needle path; (b) the pudendal nerves floating in the liquid medicine.

substantial difference ( $P < 0.05$ ). The parturients who received effective patient-controlled analgesia (1.81%) were considerably inferior to the control group (3.63%), with substantial difference ( $P < 0.05$ ).

**3.5. Comparison of Parturients' Conditions after Childbirth.** Figure 7 shows the comparison of the maternal situation after childbirth. There was no substantial difference in the time of the second stage of labor between the two groups of parturients ( $P > 0.05$ ). There was also no substantial difference in the Apgar score ( $9.56 \pm 0.34$  points) of the newborns in the experimental group and the control group ( $9.58 \pm 0.57$  points) ( $P > 0.05$ ). The satisfaction of the parturients in the experimental group ( $9.86 \pm 0.41$  points) was considerably superior to that of the control group ( $7.36 \pm 1.25$  points) ( $P < 0.05$ ). There was no substantial difference in the weight of newborns between the two groups ( $P > 0.05$ ).

**3.6. Complications.** Figure 8 shows the proportion of complications in the experimental group. In the experimental group, there were three cases of lower limb weakness (5.45%), urinary retention in two cases (3.64%), numbness of

legs and feet in eight cases (14.55%), and skin infection in one case (1.82%). No complications occurred in the control group. The incidence of complications in the experimental group was significantly lower than that in the control group.

## 4. Discussion

The subjects of this study were primiparas who underwent lateral incision through vaginal natural delivery. Due to the thick subcutaneous fat in women, the use of unilateral nerve block may not achieve the ideal analgesic effect, and the incidence of local perineal edema in women is very high. Bilateral pudendal nerve block adopted in this study can considerably improve the analgesic effect [11]. In the experimental group, ultrasound-guided pudendal nerve block was performed when the uterine orifice was about 8 cm open. At that time, pudendal nerve block did not affect the contractions of the puerpera and did not interfere with the progress of labor [3]. When the midwife performed the traditional pudendal nerve block, it was usually with the help of experience to perform the local infiltration anesthesia to relieve the pain during childbirth. Generally, the needle was inserted from the midpoint between the ischium tubercle and the anus, with the index finger and middle finger as

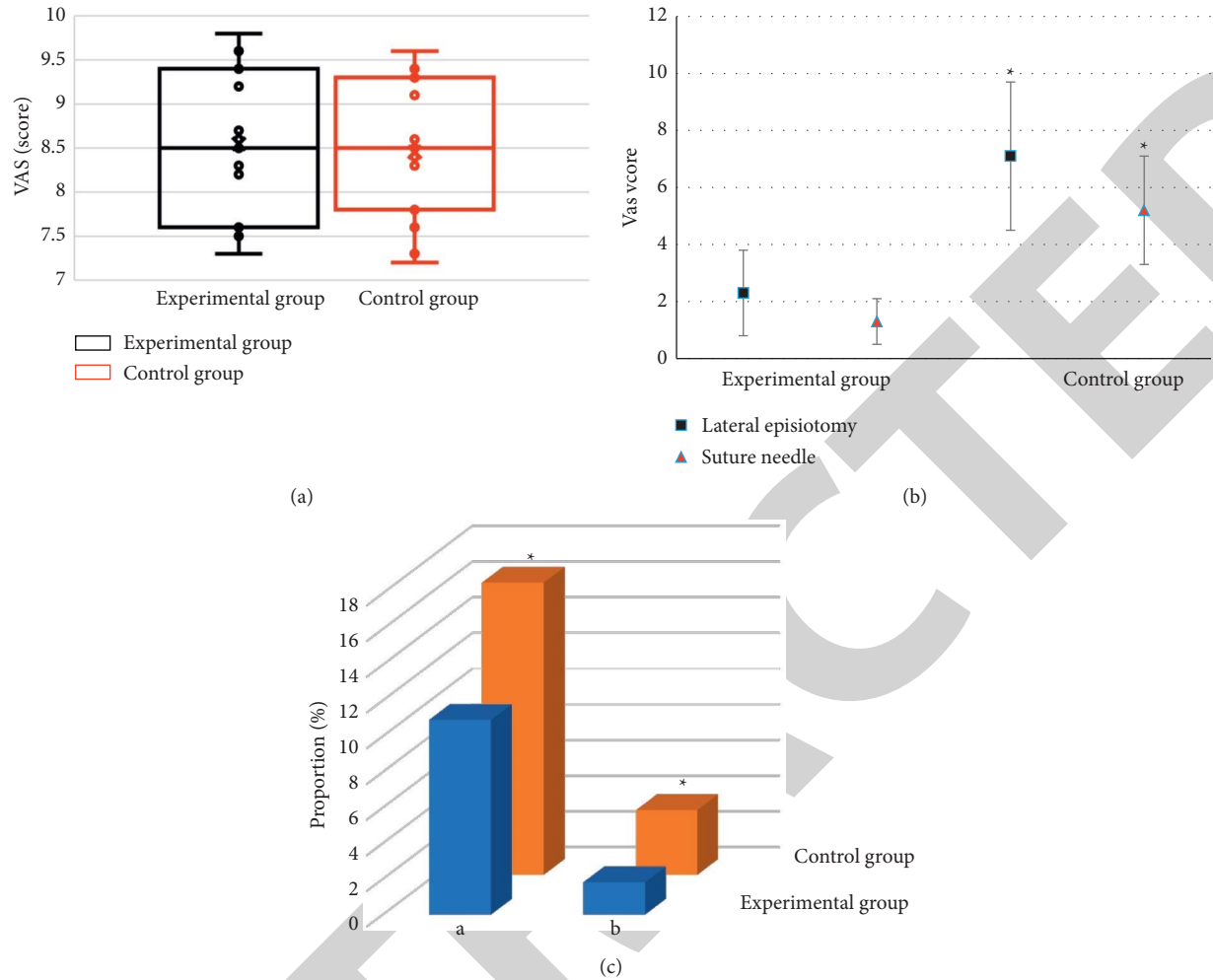


FIGURE 6: Comparison of analgesic effects in different stages of labor for parturients. (a) Comparison of VAS scores in the first stage of labor; (b) comparison of VAS scores between side cuts and stitches in the second stage of labor; (c) proportion of parturients with additional perineal local anesthesia infiltration and effective self-controlled analgesia; (a) parturients with perineal local anesthesia infiltration; (b) parturients with additional effective self-controlled analgesia. \*indicates that the difference of was substantial compared with the experimental group ( $P < 0.05$ ).

guidance, and the breakthrough was obviously felt inside the tip of the ischium spine. Local anesthetics were injected when there was no blood in the regurgitation, but ultimately the desired effect could not be achieved [12].

With the continuous development of visualization technology, many researchers are trying new approaches to ultrasound-guided pudendal nerve block. In clinical studies, the application of ultrasound in the treatment of ultrasound-guided pudendal nerve block has been consistently approved [13–15]. Ultrasound imaging is used to directly observe the movement process of the puncture needle, and it can visually show the position relationship between the needle entry route and the surrounding tissues, muscles, nerves, and blood vessels. The puncture needle can quickly and accurately reach around the block nerve plexus and observe the diffusion of local anesthetics [5]. The network model based on FSRCNN algorithm uses low-resolution images as input and uses deconvolution layer to realize upsampling, which can obtain better superresolution quality and tens of times

faster than the existing methods. Under the ultrasound imaging technology based on PSRCNN algorithm, all the parturient women in the experimental group received pudendal nerve block successfully, and the data showed that there was no substantial difference in VAS scores between the two groups before and after epidural block in the first stage of labor ( $P > 0.05$ ). This was due to pudendal nerve block failing to act on uterine contractive pain during the first generation. In the lateral resection of episiotomy in the second stage of labor, the VAS score of the experimental group and the VAS score of stitch pain were lower than those of the control group ( $P < 0.05$ ). Usually, pudendal nerve block is used for the second stage of labor. These data confirmed the obvious clinical analgesic effect of pudendal nerve block in episiotomy and perineal suture, which was consistent with the results of Li et al. [16].

In the episiotomy, there was no case of local anesthetic intoxication or nerve injury, and the pubic nerve block was successfully implemented, indicating accurate positioning of

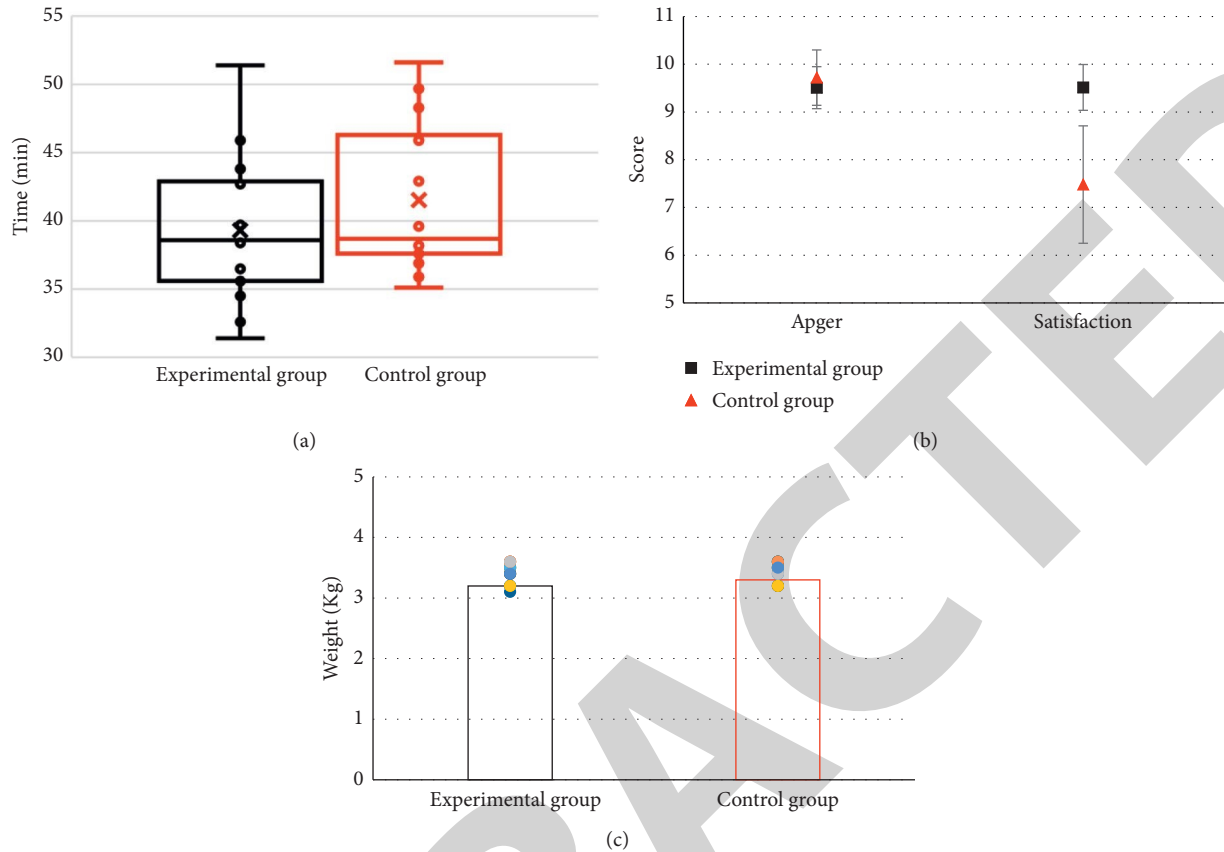


FIGURE 7: Comparison of maternal conditions after childbirth. (a) Comparison of the duration of second stage of labor; (b) neonatal Apgar score and maternal satisfaction; (c) comparison of weight of newborn. \*indicates that the difference of was substantial compared with the control group, ( $P < 0.05$ ).

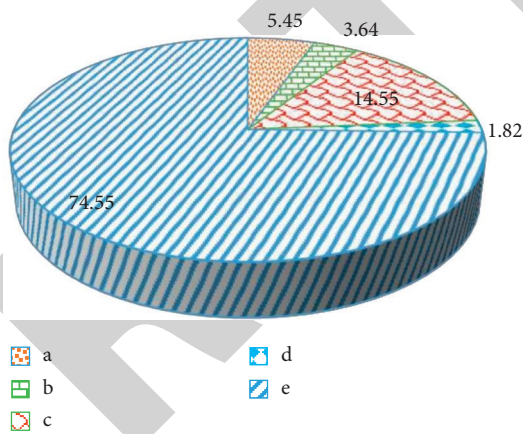


FIGURE 8: The proportion of complications in the experimental group. (a) Lower limb weakness; (b) urinary retention; (c) numbness of legs and feet; (d) skin infection; (e) no complications.

needle insertion under the guidance of ultrasound [17]. In the experimental group, there were three cases (5.45%) of lower limb weakness and eight cases (14.55%) of leg and foot numbness, but they returned to normal within 24h. No substantial difference was indicated from the prenatal level, and no sequelae occurred. Therefore, maternal lower limb weakness was not related to nerve injury. Urinary retention

occurred in two cases (3.64%). Although the pudendal nerve played a supportive role in urination, the cause of urinary retention was unclear. The incidence of complications in the experimental group was significantly lower than that in the control group, but the maternal satisfaction was much higher than that in the control group ( $P < 0.05$ ). Studies pointed out that pudendal nerve block may cause pelvic muscle relaxation, accelerate the progress of the second stage of labor, and shorten the time of the second stage of labor [18]. However, Kwon et al. [19] mentioned in the article that the time of the second stage of labor was related to many factors, such as maternal age, fetal position, and baby weight. Therefore, the sample size needs to be expanded in the later period for further verification.

### 5. Conclusion

In this study, 110 cases of primiparous women who gave birth through vagina in obstetrics and gynecology department were selected, and the optimized FSRCNN algorithm was applied to ultrasound images of pudendal nerve block of the parturients. The results showed that the optimized FSRCNN algorithm was better than the other two algorithms in terms of training time and reconstruction effect. The ultrasonic-guided pudendal nerve block had obvious analgesic effect on the second stage of labor and improved



the satisfaction of the parturients. However, the shortcomings of this study are the limited time and small sample size collected, and the VAS score used during surgery is a subjective evaluation standard for the parturients, which affects the statistical results to a certain extent. In conclusion, the optimized FSRCNN algorithm in this study has an obvious effect on the reconstruction of ultrasound images, which makes the insertion of pudendal nerve block accurate. To a great extent, it can avoid the discomfort in the process of childbirth and play an important role in the recovery after clinical obstetrics and gynecology.

## Data Availability

The data used to support the findings of this study are available from the corresponding author upon request.

## Conflicts of Interest

The authors declare no conflicts of interest.

## References

- [1] Q. Wei, Y. Xu, and L. Zhang, "Towards a universal definition of postpartum hemorrhage: retrospective analysis of Chinese women after vaginal delivery or cesarean section," *Medicine*, vol. 99, no. 33, PMID: 32872051, Article ID e21714, 2020 Aug 14.
- [2] K. Brown, J. Dormer, B. Fei, and K. Hoyt, "Deep 3D convolutional neural networks for fast super-resolution ultrasound imaging," *Medical Imaging 2019: Ultrasonic Imaging and Tomography*, vol. 10955, 2019 Feb Epub 2019 Mar 15. PMID: 32476699; PMCID: PMC7261615, Article ID 1095502.
- [3] T. Gomi, H. Hara, Y. Watanabe, and S. Mizukami, "Improved digital chest tomosynthesis image quality by use of a projection-based dual-energy virtual monochromatic convolutional neural network with super resolution," *PLoS One*, vol. 15, no. 12, PMID: 33382766; PMCID: PMC7774945, Article ID e0244745, 2020 Dec 31.
- [4] F. Özyurt, E. Sert, and D. Avci, "An expert system for brain tumor detection: fuzzy C-means with super resolution and convolutional neural network with extreme learning machine," *Medical Hypotheses*, vol. 134, 2020 Jan Epub 2019 Oct 15. PMID: 31634769, Article ID 109433.
- [5] S. Kaji and S. Kida, "Overview of image-to-image translation by use of deep neural networks: denoising, super-resolution, modality conversion, and reconstruction in medical imaging," *Radiological Physics and Technology*, vol. 12, no. 3, pp. 235–248, 2019 Sep, Epub 2019 Jun 20. PMID: 31222562.
- [6] J. Luftig, A. Dreyfuss, D. Mantuani, K. Howell, A. White, and A. Nagdev, "A new Frontier in pelvic fracture pain control in the ED: successful use of the pericapsular nerve group (PENG) block," *The American Journal of Emergency Medicine*, vol. 38, no. 12, pp. 2761.e5–2761.e9, 2020 Dec, Epub 2020 May 28. PMID: 32532621.
- [7] U. W. Lok, C. Huang, P. Gong et al., "Fast super-resolution ultrasound microvessel imaging using spatiotemporal data with deep fully convolutional neural network," *Physics in Medicine & Biology*, vol. 66, no. 7, 2021 Mar 23.
- [8] P. Naveen and P. Sivakumar, "Adaptive morphological and bilateral filtering with ensemble convolutional neural network for pose-invariant face recognition," *Journal of Ambient Intelligence and Humanized Computing*, vol. 12, no. 11, pp. 10023–10033, 2021.
- [9] B. Yao, W. Li, W. Pan et al., "Image reconstruction with a deep convolutional neural network in high-density super-resolution microscopy," *Optics Express*, vol. 28, no. 10, pp. 15432–15446, 2020 May 11, PMID: 32403571.
- [10] C. Liu, X. Wu, X. Yu, Y. Tang, J. Zhang, and J. Zhou, "Fusing multi-scale information in convolution network for MR image super-resolution reconstruction," *BioMedical Engineering OnLine*, vol. 17, no. 1, p. 114, 2018 Aug 25 PMID: 30144798.
- [11] K. Zeng, H. Zheng, C. Cai, Y. Yang, K. Zhang, and Z. Chen, "Simultaneous single- and multi-contrast super-resolution for brain MRI images based on a convolutional neural network," *Computers in Biology and Medicine*, vol. 99, pp. 133–141, 2018 Aug 1, Epub 2018 Jun 14. PMID: 29929052.
- [12] E. Sert, F. Özyurt, and A. Doğantekin, "A new approach for brain tumor diagnosis system: single image super resolution based maximum fuzzy entropy segmentation and convolutional neural network," *Medical Hypotheses*, vol. 133, 2019 Dec Epub 2019 Sep 30. PMID: 31586812, Article ID 109413.
- [13] S. Ramanarayanan, B. Murugesan, A. Kalyanasundaram et al., "MRI super-resolution using laplacian pyramid convolutional neural networks with isotropic undecimated wavelet loss," in *Proceedings of the 2020 42nd Annual International Conference of the IEEE Engineering in Medicine & Biology Society (EMBC)*, pp. 1584–1587 PMID: 33018296, Montreal, Canada, 2020 July.
- [14] T. Liu and Z. Wang, "HiCNN2: enhancing the resolution of hi-C data using an ensemble of convolutional neural networks," *Genes*, vol. 10, no. 11, p. 862, 2019 Oct 30.
- [15] X. Wang, Y. Wu, Y. Ming, and H. Lv, "Remote sensing imagery super resolution based on adaptive multi-scale feature fusion network," *Sensors*, vol. 20, no. 4, Article ID 1142, 2020 Feb 19.
- [16] B. Li, A. Keikhosravi, A. G. Loeffler, and K. W. Eliceiri, "Single image super-resolution for whole slide image using convolutional neural networks and self-supervised color normalization," *Medical Image Analysis*, vol. 68, 2021 Feb Epub 2020 Dec 9. PMID: 33359932, Article ID 101938.
- [17] A. Marques Junior, E. M. de Souza, M. Müller et al., "Improving spatial resolution of multispectral rock outcrop images using RGB data and artificial neural networks," *Sensors*, vol. 20, no. 12, Article ID 3559, 2020 Jun 23.
- [18] J. Xu, R. Zhou, W. Su et al., "Ultrasound-guided bilateral pudendal nerve blocks of nulliparous women with epidural labour analgesia in the second stage of labour: a randomised, double-blind, controlled trial," *BMJ Open*, vol. 10, no. 8, PMID: 32843515; PMCID: PMC7449485, Article ID e035887, 2020 Aug 24.
- [19] M. Kwon, S. Han, K. Kim, and S. C. Jun, "Super-resolution for improving EEG spatial resolution using deep convolutional neural network-feasibility study," *Sensors*, vol. 19, no. 23, Article ID 5317, 2019 Dec 3.